ChemComm

COMMUNICATION

View Article Online
View Journal

Cite this: DOI: 10.1039/d4cc01478b

Received 31st March 2024,
Accepted 6th June 2024

DOI: 10.1039/d4cc01478b

rsc.li/chemcomm

Assembly of a trapped valent $Ce^{III/IV}$–TCNQ complex through metal–ligand redox cooperativity†

Himanshu Gupta, Brett D. Vincenzini, Alexandra M. Bacon and Eric J. Schelter *

Complex $(Cp_3Ce^{IV})_2(TCNQ)(Ce^{III}Cp_3)_2$ (1) was prepared by reducing neutral $TCNQ^0$ (tetracyanoquinodimethane) with $Cp_3Ce(THF)$. Two types of cerium centres with a dianionic $TCNQ^{2-}$ moiety are present in 1, wherein each of the four cyano-groups are bound by a cation. Formation of this trapped-valent organocerium compound 1 is facilitated by metal–ligand redox cooperativity. Characterization of 1 was carried out using structural-, magnetometry-, and IR-spectroscopic analyses. Photophysical studies on this compound reveal Ce^{III} luminescence, and opens up avenues for promising multifunctional, mixed-valent lanthanide materials.

Metal mixed valency is of interest in reticular chemistry to achieve long-range electronic coupling and associated physical properties.[1,2] Fine-tuning of metal frontier orbital overlap and associated redox potentials can afford discovery of emergent phenomena in molecule-based materials, tuning that is typically not possible in intermetallic nor other solid-state materials.[3–5] For example, redox active organics such as pyrazine have been shown to induce variable magnetic and conducting properties in materials comprising transition metal salts.[6–8] Lanthanide compounds that are otherwise dominated by the trivalent oxidation state can exhibit notable behaviours in formally divalent or tetravalent materials upon combining with suitable electron donors/acceptors.[9–11]

Electron acceptors such as fullerenes, TCNQ (tetracyanoquinodimethane), TCNE (tetracyanoethylene) and others have been shown to assemble notable structures and associated, collective properties through charge transfer processes.[12–14] TCNQ and TCNE offer multiple accessible redox states and four terminal cyano-functionalities that bind metal coordination sites to assemble magnetic, conducting and multifunctional materials.[5,15,16] Mixed valent ferrocene-TCNQ materials comprising π–π interactions have also been assembled by charge transfer processes.[17] On the other hand, redox assembly of lanthanide based TCNQ materials remain unexplored with the exception of ytterbocene, $(C_5Me_5)_2Yb^{II}(THF)_2$, which undergoes an unusual oxidative reorganization with TCNQ to form the Yb^{III} dimer, $[(C_5Me_5)_2Yb^{III}(CH_3CN)\{(\mu\text{-}CN)_2(C_6H_4)(CN)_2\}]_2$.[18] A previous report of a ribbon-like coordination polymer of Ce^{III} and $TCNQX_2$ X = –Cl, –Br showed notable magnetic coercivity, but was not formed through redox processes.[13]

Among organometallic lanthanide complexes, cerium offers relatively mild and tunable $Ce^{III/IV}$ oxidation potentials,[19,20] and isolable tetravalent compounds.[21–26] Tris(cyclopentadienyl) cerium(III) complexes have previously been shown to be a useful platform to access organocerium(IV) compounds: Cp_3Ce–X, X = –halides, –alkoxides, and –aryloxides.[27–29] As such, we expected that this platform could be used for molecule-based materials with multifunctional charge transfer properties if assembled with suitable organic acceptors. Our group recently reported that $(C_5Me_4H)_3Ce$ reacts with C_{60} to form $[(C_5Me_4H)_3Ce]_2 \cdot C_{60}$ where intermolecular interactions promoted the emergence of Mott insulator behaviour reminiscent of Ce_2O_3.[30] In the current work, we provide an initial demonstration that high valent, organocerium-based materials can be achieved with metal–ligand redox cooperativity using the organic acceptor TCNQ.

The first reduction of $TCNQ^0$ reportedly occurs at $E_{1/2}$ = –0.34 V *versus* Fc in THF while the second reduction occurs at $E_{1/2}$ = –1.01 V.[31] We set out to explore organocerium-based material by reducing TCNQ with $Cp_3Ce(THF)$, the latter of which shows an oxidation potential of $E_{1/2}$ = –0.26 V *versus* Fc in THF.[29] Reaction of $Cp_3Ce(THF)$ with TCNQ in toluene results in immediate precipitation of a brown solid. Using the tetramethylated precursor: $(C_5Me_4H)_3Ce$ towards the goal of preparing a compound with increased solubility, does not show any color change or precipitation upon reaction with $TCNQ^0$ in toluene. We postulate that the larger steric demand offered by three $C_5Me_4H^-$ ligands prevent interaction with $TCNQ^0$ to initiate the redox reaction. An optimized synthesis of the

P. Roy and Diana T. Vagelos Laboratories, Department of Chemistry, University of Pennsylvania, 231 South 34th Street, Philadelphia, Pennsylvania 19104, USA. E-mail: schelter@sas.upenn.edu

† Electronic supplementary information (ESI) available: Synthetic Details, characterization, additional magnetometry, vibrational spectroscopy, and X-ray crystallographic data. CCDC 2343799. For ESI and crystallographic data in CIF or other electronic format see DOI: https://doi.org/10.1039/d4cc01478b

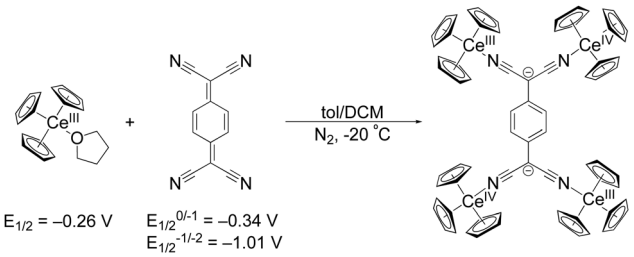

Scheme 1 Synthetic conditions for **1** from $Cp_3Ce(THF)$ and TCNQ along with their respective redox potentials *versus* Fc in THF.

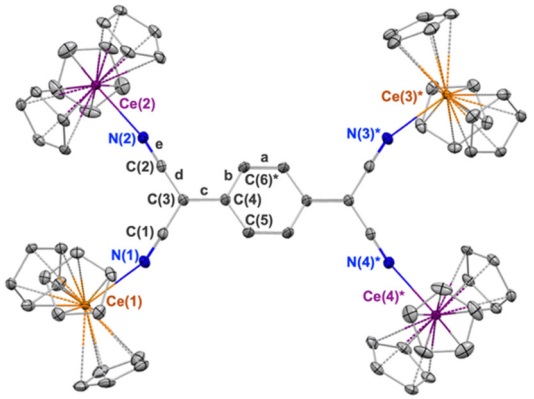

Fig. 1 Thermal ellipsoid plot of **1** shown at the 30% probability level. Ce^{III} centers are shown in orange and Ce^{IV} in purple color. The * indicates atoms at equivalent position (–*x*,1–*y*,1–*z*). Hydrogen atoms and co-crystalized toluene molecules are omitted for clarity.

former reaction with $Cp_3Ce(THF)$ produced a crystalline, brown-black material, suitable for single crystal X-ray diffraction analysis, in 71% yield (see ESI† for details). The isolated material was insoluble in toluene, DCM, and Et_2O at RT. Addition of THF and acetonitrile to the solid **1** produces yellow coloration, likely due to reductive decomposition. Notably, single crystal X-ray diffraction shows a neutral tetrameric complex $(Cp_3Ce^{IV})_2(TCNQ)(Ce^{III}Cp_3)_2$ (**1**) with the $TCNQ^{2-}$ ligand in the doubly reduced state (Scheme 1).

The X-ray diffraction data for **1** are shown in the Table 1. The tetrameric $TCNQ^{2-}$ complex consists of two, structurally distinct, types of cerium centres. The Ce–N and Ce–Cp(centroid) bond distances at Ce(1) and Ce(3)* are 2.558(3) Å and 2.558(avg.) Å respectively, the latter of which is consistent with the structure of the previously reported Cp_3Ce^{III}–$OC(NMe_2)_2$, 2.576(avg.) Å.[32] These same bond distances at Ce(2) and Ce(4)* are 2.414(3) Å and 2.458(avg.) Å, respectively, distances that more closely resemble those of $Cp_3Ce^{IV}Cl$ with Ce–Cp(centroid) distance 2.460(avg.) Å.[27] The redox state of the $TCNQ^{2-}$ ligand in **1** was evaluated by examining the bond length *c* (Fig. 1), where a change to the benzenoid form upon reduction is expressed through an elongation of that bond compared to neutral TCNQ. In **1**, this bond length is 1.468(3) Å which is longer than the 1.374(3) Å observed in the structure of neutral TCNQ.[33] The bond length *c* is also used in the Kistenmacher relationship calculation to estimate the charge distribution on TCNQ.[34] (see ESI†). For **1**, the net calculated charge on TCNQ is −2.19.

A notable feature of **1** is the bond angles described by the atoms: Ce–N≡C. For the Ce(2) and Ce(4)* sites comprising the tetravalent oxidation state, more linear Ce(IV)–N≡C bond angles of 168.5(3)° are observed. The Ce(1) and Ce(3)* sites exhibit more bent Ce(III)–N≡C bond angles of 159.9(3)°, presumably due to the weaker association of the cyano groups with the cerium(III) cations. Overall, based on the structural investigation, **1** comprises two cerium(III) cations and two cerium(IV) cations and is best described as a trapped-valent complex, class I under the Robin–Day classification.[37]

TCNQ vibrational signatures are sensitive to the extent of reduction of this moiety in molecules and materials. IR spectra were collected and compared with neutral TCNQ crystals and **1** in a KBr matrix. Compound **1** shows characteristic stretching frequencies associated with the cyano groups at 2098 and 2177 cm^{-1} (Table 1) whereas neutral TCNQ shows a single feature at 2223 cm^{-1}. This evident decrease in frequency is attributed to $2e^-$ reduction of TCNQ moiety in **1** as reported previously.[38] Attempts to perform Raman measurements of **1** were unsuccessful due to a consistently poor signal-to-noise ratio.

Malischewski and co-workers recently reported that coordination of $B(C_6F_5)_3$ to TCNQ shifted the first reduction potential of the latter by 1.2 V to 0.9 V *versus* Fc in CH_2Cl_2.[39] We and others have previously shown such Lewis acid promoted potential shift (LAPPS) of organic acceptors using trivalent lanthanides.[35,40] For example, we demonstrated LAPPS by cerium coordination and concomitant reduction of *para*-benzoquinone using $[\{Li_3(thf)_4\}\{(BINOLate)_3Ce(thf)\}]$.[41] Similarly, **1** evidently assembles from a Lewis acid effect of Ce^{III} bonding that shifts the redox potentials of the Cp_3Ce donor and TCNQ acceptor, and relatively covalent bonding of Ce^{IV} coordination. The operative Lewis acid-assisted coordination significantly lowers the reduction potentials of TCNQ and concurrently reduces it to assemble the trapped valent cerium complex **1**. This chemistry is reminiscent of transition metals based TCNQ reduction that has not been previously reported for lanthanides.[42]

Table 1 Bond length and cyano vibrational frequency comparison for **1** and reported $TCNQ^{0/\bullet-/2-}$ materials

	Bond '*c*' (Å)	M–N (Å)	ν_{CN} (cm^{-1})	M–N≡C (°)
1 (M = Ce)	1.469 (5)	2.414(3), 2.558(3)	2098, 2177	168.5(3), 159.9(3)
$TCNQ^0$ (ref. 35)	1.374(3)	n/a	2223	n/a
$TCNQ^{\bullet-}$ (ref. 17, M = Ce)	1.400–1.432	2.654–2.666	2165, 2198	168.7(3), 149.0(3), 171.4(3)
$TCNQ^{2-}$ (ref. 36, M = Zn)	1.472(5)	2.160(3)–2.167(3)	2121, 2194	159.26(3), 158.21(3)

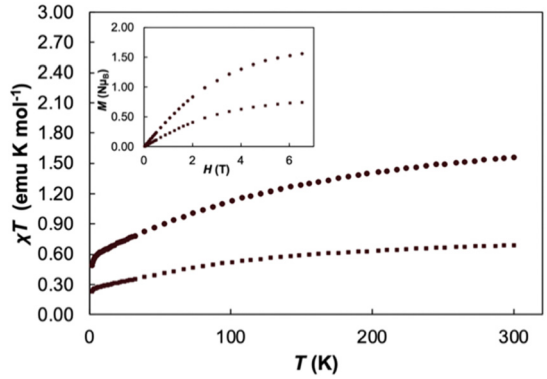

Fig. 2 Variable temperature χT measurements of $Cp_3Ce(THF)$ (square markers) and **1** (circle markers) at 2*T*, variable field magnetization experiments (inset) conducted at T = 2 K.

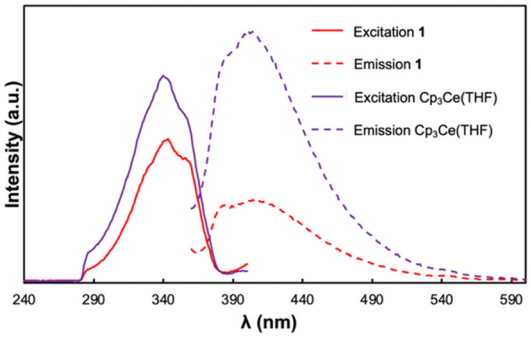

Fig. 3 Photoluminescence spectra of **1** (red) and $Cp_3Ce(THF)$ (purple) as a suspension in toluene and a 0.005 mM solution respectively. The excitation spectra at 420 nm emission are shown as solid traces. The emission spectra at 340 nm excitation are shown as dashed traces.

Variable temperature magnetic susceptibility data performed at 2 T and variable field magnetization saturation experiments performed at 2 K were recorded for **1** to further verify the redox assignment of the cerium cations and TCNQ (Fig. 2). For $Cp_3Ce(THF)$, the $\chi_M T$ value is 0.68 emu K mol^{-1} at 300 K and slowly decreases to 0.25 emu K mol^{-1} at 2 K, similar to the reported value for $Cp_3CeOP(NMe_2)_3$.[36] For **1**, the $\chi_M T$ value is 1.56 emu K mol^{-1} at 300 K and slowly decreases to 0.49 emu K mol^{-1} at 2 K. This data falls in the expected range for two non-interacting Ce^{III} ions (1.60 emu K mol^{-1}) and helps to confirm the presence of two Ce^{III} cations in **1**. With decreasing temperature, the $\chi_M T$ value decreases slowly and drops to 0.50 emu K mol^{-1} at 2 K. This decrease in the χT product is likely due to thermal depopulation of the cerium(III) Kramers doublets or weak antiferromagnetic coupling. A field dependent magnetization saturation experiment showed a value of M = 1.59μ_B at 2 K at an applied field of 7 T, which further supports the assignment of two cerium(III) centres in **1**.[43]

To further interrogate the photophysical properties of **1**, photoluminescence spectra were collected on (only poorly soluble) suspensions of the compound in toluene (Fig. 3). With excitation at 340 nm, a broad emission band was observed with λ_{max} = 414 nm. The excitation spectrum of **1**, collected between 230 and 380 nm, contains a broad excitation band with λ_{max} = 343 nm and a prominent shoulder located at 360 nm. The separation of λ_{max} and the lower energy shoulder is 1377 cm^{-1} which falls in the range of peak separations commonly observed for cerium(III) 5d → 4f transitions between the ^2D excited state and $^2F_{5/2}$ and $^2F_{7/2}$ ground state manifold.[44] The Stokes shift for **1** was determined to be 54 nm (0.45 eV) which is comparable to those shifts reported for other luminescent cerium(III) compounds.[45] Given that the luminescence profile of **1** resembles those observed for reported Ce(III) 5d → 4f emissions, we tentatively attribute the observed luminescence features to electronic transitions at the cerium(III) sites of **1**.

Previous studies of the photophysical properties of neutral TCNQ revealed that it exhibits solvent dependent photoluminescent behaviour.[46] While TCNQ was not luminescent in toluene, the starting $Cp_3Ce(THF)$ complex exhibited a similar luminescence profile to **1** and resembled the spectra previously reported in THF.[47] The excitation spectrum was essentially indistinguishable from that of **1** with an identical λ_{max} value and prominent shoulder at 343 and 360 nm respectively. Notwithstanding, the emission band of $Cp_3Ce(THF)$ obtained upon excitation at 340 nm occurred at slightly higher energy with the λ_{max} = 403 nm. As such, $Cp_3Ce(THF)$ exhibits a smaller Stokes shift than that of **1** (43 nm, 0.36 eV). Our group has previously demonstrated that the Stokes shift in cerium(III) emitters is correlated with the degree of nonradiative vibrational losses of energy in the emissive state(s).[48] The results therefore indicate that **1** undergoes greater vibrational relaxation in the ^2D excited state compared with the mononuclear $Cp_3Ce(THF)$ complex.

A synthetic pathway for cerium coordination-induced double reduction of TCNQ has been described. This strategy can be used to assemble molecule-based materials comprising reduced organics with otherwise poorly matched donor–acceptor redox potentials. Currently, studies of a range of these materials with various metals and Cp-substituents, and studies of their electronic structures towards multi-functional materials are underway in our laboratory.

We gratefully acknowledge the U.S. Department of Energy under Award DE-SC0020169 for support of this work. H. G. also acknowledges the Vagelos Institute for Energy Science and Technology for a graduate fellowship. And E. J. S. also thanks the University of Pennsylvania for financial support. We also thank the JASCO facility for Spectroscopic Excellence in the Chemistry Department at the University of Pennsylvania for access to the Raman spectrometer used in this work.

Data availability statement

Data supporting this article have been included as part of the ESI.† Crystallographic data for **1** have been deposited at the CCDC under accession number 2343799 and can be obtained from **https://www.ccdc.cam.ac.uk/structures**.

Conflicts of interest

There are no conflicts to declare.

Notes and references

1 R. Murase, C. F. Leong and D. M. D'Alessandro, *Inorg. Chem.*, 2017, **56**, 14373–14382.
2 L. E. Darago, M. L. Aubrey, C. J. Yu, M. I. Gonzalez and J. R. Long, *J. Am. Chem. Soc.*, 2015, **137**, 15703–15711.
3 J. Xie, S. Ewing, J.-N. Boyn, A. S. Filatov, B. Cheng, T. Ma, G. L. Grocke, N. Zhao, R. Itani, X. Sun, H. Cho, Z. Chen, K. W. Chapman, S. N. Patel, D. V. Talapin, J. Park, D. A. Mazziotti and J. S. Anderson, *Nature*, 2022, **611**, 479–484.
4 L. S. Xie, G. Skorupskii and M. Dincă, *Chem. Rev.*, 2020, **120**, 8536–8580.
5 A. E. Thorarinsdottir and T. D. Harris, *Chem. Rev.*, 2020, **120**, 8716–8789.
6 K. S. Pedersen, P. Perlepe, M. L. Aubrey, D. N. Woodruff, S. E. Reyes-Lillo, A. Reinholdt, L. Voigt, Z. Li, K. Borup, M. Rouzières, D. Samohvalov, F. Wilhelm, A. Rogalev, J. B. Neaton, J. R. Long and R. Clérac, *Nat. Chem.*, 2018, **10**, 1056–1061.
7 P. Perlepe, I. Oyarzabal, A. Mailman, M. Yquel, M. Platunov, I. Dovgaliuk, M. Rouzières, P. Négrier, D. Mondieig, E. A. Suturina, M.-A. Dourges, S. Bonhommeau, R. A. Musgrave, K. S. Pedersen, D. Chernyshov, F. Wilhelm, A. Rogalev, C. Mathonière and R. Clérac, *Science*, 2020, **370**, 587–592.
8 P. Perlepe, I. Oyarzabal, L. Voigt, M. Kubus, D. N. Woodruff, S. E. Reyes-Lillo, M. L. Aubrey, P. Négrier, M. Rouzières, F. Wilhelm, A. Rogalev, J. B. Neaton, J. R. Long, C. Mathonière, B. Vignolle, K. S. Pedersen and R. Clérac, *Nat. Commun.*, 2022, **13**, 5766.
9 M. A. Dunstan, A. S. Manvell, N. J. Yutronkie, F. Aribot, J. Bendix, A. Rogalev and K. S. Pedersen, *Nat. Chem.*, 2024, **16**, 735–740.
10 L. Münzfeld, S. Gillhuber, A. Hauser, S. Lebedkin, P. Hädinger, N. D. Knöfel, C. Zovko, M. T. Gamer, F. Weigend, M. M. Kappes and P. W. Roesky, *Nature*, 2023, **620**, 92–96.
11 C. H. Booth, M. D. Walter, M. Daniel, W. W. Lukens and R. A. Andersen, *Phys. Rev. Lett.*, 2005, **95**, 267202.
12 J. Arvanitidis, K. Papagelis, S. Margadonna, K. Prassides and A. N. Fitch, *Nature*, 2003, **425**, 599–602.
13 M. Ballesteros-Rivas, H. Zhao, A. Prosvirin, E. W. Reinheimer, R. A. Toscano, J. Valdés-Martínez and K. R. Dunbar, *Angew. Chem., Int. Ed.*, 2012, **51**, 5124–5128.
14 J. G. Park, D. E. Jaramillo, Y. Shi, H. Z. H. Jiang, H. Yusuf, H. Furukawa, E. D. Bloch, D. S. Cormode, J. S. Miller, T. D. Harris, E. Johnston-Halperin, M. E. Flatté and J. R. Long, *ACS Cent. Sci.*, 2023, **9**, 777–786.
15 B. F. Abrahams, R. W. Elliott, T. A. Hudson, R. Robson and A. L. Sutton, *CrystEngComm*, 2018, **20**, 3131–3152.
16 Ö. Üngör and M. Shatruk, *Polyhedron*, 2020, **177**, 114254.
17 T. Mochida, Y. Funasako, S. Yamazaki and H. Mori, *Eur. J. Inorg. Chem.*, 2014, 3920–3926.
18 A. A. Trifonov, I. D. Gudilenkov, G. K. Fukin, A. V. Cherkasov and J. Larionova, *Organometallics*, 2009, **28**, 3421–3425.
19 N. A. Piro, J. R. Robinson, P. J. Walsh and E. J. Schelter, *Coord. Chem. Rev.*, 2014, **260**, 21–36.
20 C. Uruburo, D. M. R. Y. P. Rupasinghe, H. Gupta, R. M. Knieser, L. M. Lopez, M. H. Furigay, R. F. Higgins, P. Pandey, M. R. Baxter, P. J. Carroll, M. Zeller, S. C. Bart and E. J. Schelter, *Inorg. Chem.*, 2024, **63**(21), 9418–9426.
21 G. B. Panetti, D.-C. Sergentu, M. R. Gau, P. J. Carroll, J. Autschbach, P. J. Walsh and E. J. Schelter, *Nat. Commun.*, 2021, **12**, 1713.
22 Y. Qiao, H. Yin, L. M. Moreau, R. Feng, R. F. Higgins, B. C. Manor, P. J. Carroll, C. H. Booth, J. Autschbach and E. J. Schelter, *Chem. Sci.*, 2021, **12**, 3558–3567.
23 J. A. Bogart, C. A. Lippincott, P. J. Carroll, C. H. Booth and E. J. Schelter, *Chem. - Eur. J.*, 2015, **21**, 17850–17859.
24 N. T. Rice, I. A. Popov, D. R. Russo, T. P. Gompa, A. Ramanathan, J. Bacsa, E. R. Batista, P. Yang and H. S. La Pierre, *Chem. Sci.*, 2020, **11**, 6149–6159.
25 I. J. Casely, S. T. Liddle, A. J. Blake, C. Wilson and P. L. Arnold, *Chem. Commun.*, 2007, 5037–5039.
26 A. J. Gremillion, J. Ross, X. Yu, P. Ishtaweera, R. Anwander, J. Autschbach, G. A. Baker, S. P. Kelley and J. R. Walensky, *Inorg. Chem.*, 2024, **63**(21), 9602–9609.
27 P. Dröse, A. R. Crozier, S. Lashkari, J. Gottfriedsen, S. Blaurock, C. G. Hrib, C. Maichle-Mössmer, C. Schädle, R. Anwander and F. T. Edelmann, *J. Am. Chem. Soc.*, 2010, **132**, 14046–14047.
28 D. Schneider, N. Harmgarth, F. T. Edelmann and R. Anwander, *Chem. - Eur. J.*, 2017, **23**, 12243–12252.
29 L. Hirneise, J. Langmann, G. Zitzer, L. Ude, C. Maichle-Mössmer, W. Scherer, B. Speiser and R. Anwander, *Organometallics*, 2021, **40**, 1786–1800.
30 P. Pandey, X. Wang, H. Gupta, P. W. Smith, E. Lapsheva, P. J. Carroll, A. M. Bacon, C. H. Booth, S. G. Minasian, J. Autschbach, E. Zurek and E. J. Schelter, *ACS Appl. Mater. Interfaces*, 2024, **16**(14), 17857–17869.
31 E. J. Schelter, D. E. Morris, B. L. Scott, J. D. Thompson and J. L. Kiplinger, *Inorg. Chem.*, 2007, **46**, 5528–5536.
32 Â. Domingos, N. Marques, A. Pires de Matos, M. G. Silva-Valenzuela and L. B. Zinner, *Polyhedron*, 1993, **12**, 2545–2549.
33 R. E. Long, R. A. Sparks and K. N. Trueblood, *Acta Crystallogr.*, 1965, **18**, 932–939.
34 A. L. Sutton, B. F. Abrahams, D. M. D'Alessandro, R. W. Elliott, T. A. Hudson, R. Robson and P. M. Usov, *CrystEngComm*, 2014, **16**, 5234–5243.
35 S. Fukuzumi and K. Ohkubo, *Chem. - Eur. J.*, 2000, **6**, 4532–4535.
36 E. M. Aricó, B. Kanellakopulos, C. Apostolidis and L. B. Zinner, *J. Alloys Compd.*, 1998, **275–277**, 798–800.
37 M. B. Robin and P. Day, in Mixed Valence Chemistry-A Survey and Classification, *Advances in Inorganic Chemistry and Radiochemistry*, ed. Emeléus, H. J., Sharpe, A. G., Academic Press, 1968, vol. 10, pp. 247–422.
38 S. Shimomura, R. Matsuda, T. Tsujino, T. Kawamura and S. Kitagawa, *J. Am. Chem. Soc.*, 2006, **128**, 16416–16417.
39 P. A. Albrecht, S. M. Rupf, M. Sellin, J. Schlögl, S. Riedel and M. Malischewski, *Chem. Commun.*, 2022, **58**, 4958–4961.
40 S. Fukuzumi, *Org. Biomol. Chem.*, 2003, **1**, 609–620.
41 J. R. Robinson, C. H. Booth, P. J. Carroll, P. J. Walsh and E. J. Schelter, *Chem. - Eur. J.*, 2013, **19**, 5996–6004.
42 R. Gross and W. Kaim, *Angew. Chem., Int. Ed. Engl.*, 1987, **26**, 251–253.
43 O. Kahn, *Molecular Magnetism*, Wiley, 1993.
44 P. Pandey, Q. Yang, M. R. Gau and E. J. Schelter, *Dalton Trans.*, 2023, **52**, 5909–5917.
45 Y. Qiao and E. J. Schelter, *Acc. Chem. Res.*, 2018, **51**, 2926–2936.
46 H. Tamaya, H. Nakano and T. Iimori, *J. Lumin.*, 2017, **192**, 203–207.
47 P. N. Hazin, J. W. Bruno and H. G. Brittain, *Organometallics*, 1987, **6**, 913–918.
48 Y. Qiao, D.-C. Sergentu, H. Yin, A. V. Zabula, T. Cheisson, A. McSkimming, B. C. Manor, P. J. Carroll, J. M. Anna, J. Autschbach and E. J. Schelter, *J. Am. Chem. Soc.*, 2018, **140**, 4588–4595.

